Crystal Structure and Magnetic Behavior of [(C₂H₅)₄N]₂Cu₅Cl₁₂. A Novel Two-Dimensional Copper(II) Halide Network Derived from the CuCl₂ Structure

**José A. Ayllón,*,† Isabel C. Santos,† Rui T. Henriques,† Manuel Almeida,*,†
Luís Alcácer,‡ and Maria T. Duarte‡**

Departamento de Química, Instituto Tecnológico e Nuclear, P-2686 Sacavém Codex, Portugal, and
Departamento de Engenharia Química, Instituto Superior Técnico, P-1096 Lisboa Codex, Portugal

A new chlorocuprate(II), [(C₂H₅)₄N]₂Cu₅Cl₁₂, was prepared by reaction of CuCl₂·2H₂O and (C₂H₅)₄NCl in 1,1,2-trichloroethane−ethanol followed by water−ethanol evaporation. The crystal structure, solved by single-crystal X-ray diffraction at room temperature, was found to be triclinic, space group $P\bar{1}$, with cell parameters $a = 8.9123(9)$ Å, $b = 11.0690(8)$ Å, $c = 11.2211(9)$ Å, $\alpha = 118.766(6)°$ $\beta = 109.041(8)°$, $\gamma = 97.465(7)°$, and $Z = 1$, and consists of a two-dimensional network of $[(Cu_5Cl_{12})^{2-}]_\infty$ parallel to the *a, b* plane, alternating with layers of the organic cations along *c*. The anionic sheets are built up by aggregation of infinite zigzag chains of alternating tetranuclear and mononuclear subsequences. This structure can be related to the anhydrous CuCl₂ structure by systematic removal of $(Cu_2Cl_6)^{2+}$ fragments. The magnetic susceptibility of this compound can be described by a simple model, suggested by the structural data, that considers independent contributions of linear tetramers, with antiferromagnetically coupled pairs of copper atoms ($J_1/k = -64(2)$ K), and almost magnetically isolated Cu(II) centers, that obey a Curie−Weiss law with a $\Theta = -2.7(8)$ K.

Introduction

The structural properties of the large number of copper(II) halides are interesting, primarily due to the wide variety of stereochemical arrangements observed,[1,2] which can be viewed as models for the studies of magnetic properties of more complex systems.[3] The flexibility of the Cu(II) coordination sphere and the nonstereospecific nature of the halide anions, modulated by the size and hydrogen bonding properties of the cation, allow the large span of geometries observed.[4] The identification of all the factors which influence the stereochemistry of those compounds has been discussed on basis of the Jahn−Teller effect, crystal field stabilization, both the halide−halide and halide−environment electrostatic interactions, and crystal packing effects.[1]

Some of these structures are unique, but it is possible to order most of them in families. Among them the pseudoplanar oligomers with formula $A_2Cu_nX_{2n+2}$ (or $A_2Cu_nX_{2n}L_2$ or A_2-$Cu_nX_{2n+1}L$; where A is a monocation, X is a chloride or a bromide, and L is a neutral ligand) belong to an important family of structures.[5] In this family the oligomers typically aggregate by semicoordinative bonds in a large variety of stacking patterns, extensively studied by Willett et al.[5−16] Willett, on the basis of a few real examples, has also recently discussed the

hypothetical existence of another wide family of structures, derived from the layered CuCl₂ structure by removal of positive fragments.[2]

In this paper we report the synthesis and characterization a new chlorocuprate(II) with stoichiometry [(C₂H₅)₄N]₂Cu₅Cl₁₂, to the best of our knowledge the first one with this stoichiometry between halide anions and copper(II) cations. Although this stoichiometry could a priori suggest that we have found another member in the family of the pseudoplanar oligomers with formula $(Cu_nCl_{2n+2})^{2-}$, the X-ray crystal analysis reveals a structure not only different from a stack of pentamers but also distinctly different from the previously known halocuprates-(II), although still related to the parent CuCl₂ structure.

Experimental Section

Preparation of [(C₂H₅)₄N]₂Cu₅Cl₁₂. CuCl₂·2H₂O (263 mg, 1.54 mmol) and (C₂H₅)₄NCl (102 mg, 0.62 mmol) were dissolved in absolute ethanol (20 mL), and 1,1,2-trichloroethane (30 mL) was added. The green solution was heated to the boiling temperature, and the solvent was allowed to evaporate until a final volume of approximately 25 mL was reached, while the color changed to dark-red. This solution was then allowed to cool to room temperature in a sealed vessel, precipitating a dark-orange crystalline and moisture-sensitive solid. After filtration under argon, the solid was washed with dry dichloromethane and hexane and kept away from atmospheric moisture. It should be noted that although water-containing starting materials were used, this synthetic procedure leads to water elimination, by evaporation as an ethanol−water azeotrope. Single crystals adequate for X-ray diffraction analysis were directly obtained. This synthesis is critically dependent on the rate of evaporation and final volume obtained; if the concentration is insufficient, no precipitate is obtained; if the solution is too concentrated, the precipitation is very fast giving a very fine and poorly crystallized, or even amorphous, powder that is extremely moisture sensitive. When this happened it was possible to redissolve the solid, adding more ethanol, and to concentrate again the solution in order to

---

† Instituto Tecnológico e Nuclear.
‡ Instituto Superior Técnico.
⊗ Abstract published in *Advance ACS Abstracts,* December 1, 1995.
(1) Willett, R. D. *Coord. Chem. Rev.* **1991,** *109,* 181.
(2) Weise, S.; Willett, R. D. *Acta Crystallogr., Sect C* **1993,** *C49,* 283.
(3) Blanchette, J. T.; Willett, R. D. *Inorg. Chem.* **1988,** *27,* 843.
(4) Bond, M. R.; Willett, R. D.; Rubenacker, G. V. *Inorg. Chem.* **1990,** *29,* 2713.
(5) Willett, R. D. *Acta Crystallogr., Sect A* **1993,** *A49,* 613.
(6) Willett, R. D. *Acta Crystallogr., Sect B* **1988,** *B44,* 503.
(7) Bond, M. R.; Willett, R. D. *Acta Crystallogr., Sect C* **1991,** *C47,* 1084.
(8) Bond, M. R.; Willett, R. D. *Acta Crystallogr., Sect C* **1991,** *C47,* 1973.
(9) Bond, M. R.; Willett, R. D. *Acta Crystallogr., Sect C* **1992,** *C48,* 1189.
(10) Fletcher, R.; Hansen, J. J.; Livermore, J.; Willett, R. D. *Inorg. Chem.* **1983,** *22,* 330.
(11) Colombo, A.; Menabue, L.; Motori, A.; Pellacani, G. C.; Porzio, W.; Sandrolini, F.; Willett, R. D. *Inorg. Chem.* **1985,** *24,* 2900.
(12) Halvorson, K. E.; Grigereit, T.; Willett, R. D. *Inorg. Chem.* **1987,** *26,* 1716.

(13) Grigereit, T. E.; Ramakrishna, B. L.; Place, H.; Willett, R. D.; Pellacani, G. C.; Manfredini, T.; Menabue, L.; Bonamartini-Corradi, A.; Battaglia, L. P. *Inorg. Chem.* **1987,** *26,* 2235.
(14) Bond, M. R.; Willett, R. D. *Inorg. Chem.* **1989,** *28,* 3267.
(15) Willett, R. D.; Bond, M. R.; Pon, G. *Inorg. Chem.* **1990,** *29,* 4160.
(16) Geiser, U.; Willett, R. D.; Lindbeck, M.; Emerson, K. *J. Am. Chem. Soc.* **1986,** *108,* 1173.

Table 1. Crystallographic Data for $[(C_2H_5)_4N]_2Cu_5Cl_{12}$

formula	$C_{16}H_{40}N_2Cl_{12}Cu_5$	d_{calc}, g/cm³	1.937
fw	501.80	T, K	293(2)
a, Å	8.9123(9)	wavelength, Å	0.71069
b, Å	11.0690(8)	μ(Mo Kα), cm⁻¹	39.84
c, Å	11.2211(9)	space group	$P\bar{1}$
α, deg	118.766(6)	V, Å³	860.52(13)
β, deg	109.041(8)	R^a	0.0525
γ, deg	97.465(7)	$R_w{}^b$	0.1156
Z	1	S^c	1.093

$^a R = \sum||F_o| - |F_c||/\sum|F_o|.$ $^b R_w = [\sum[w(F_o{}^2 - F_c{}^2)^2]/\sum[w(F_o{}^2)^2]]^{1/2}.$
$^c S = \sum[[w(F_o{}^2 - F_c{}^2)^2]/(n - p)]^{1/2};$ $w = 1/[\sigma^2 F_o{}^2 + (0.0722P)^2 + 0.15P];$ $P = (\max(F_o{}^2 + 2F_c{}^2))/3.$

obtain a crystalline product by the same cooling procedure already mentioned. Due to the critical dependence on the evaporation process described above, the yield is quite variable but more than 40% was achieved in many cases. The elemental analysis using a Perking-Elmer 240 elemental analyzer at the analytical service of our laboratory gave the following results. Anal. Calcd for $C_{16}Cl_{12}Cu_5H_{40}N_2$: N, 2.79; C, 19.15; H, 4.02. Found: N, 2.89; C, 19.09; H, 3.90.

X-ray Crystallography. A dark-orange crystal of approximate dimensions $0.6 \times 0.4 \times 0.04$ mm³ was mounted in a glass capillary on a goniometer head. X-ray data were collected at room temperature on an Enraf-Nonius CAD-4 automatic diffractometer equipped with graphite monochromated Mo Kα radiation ($\lambda = 0.710\,69$ Å). Unit cell dimensions and a crystal orientation matrix were obtained from least-squares refinement of the setting angles of 25 reflections in the $10 < \theta < 14°$ range. The unit cell was identified as triclinic, space group $P\bar{1}$. This choice was confirmed by the solution and the successful refinement of the structure. The data set was collected in a $\omega-2\theta$ scan mode [$\Delta\omega = (0.80 + 0.35 \tan\theta)°$]. The intensities were corrected for Lorentz and polarization effects, and an empirical absorption correction (ψ scan) was made The Enraf-Nonius SDP Library was used for data reduction (maximum and minimum transmission factors were 0.998 and 0.554). The structure was solved by standard Patterson methods using SHELX86,[17] and subsequently completed by Fourier recycling using SHELXL93.[18] All non-hydrogen atoms were refined anisotropically. The hydrogen atoms were set in calculated positions. Final refinement on $F_o{}^2$ by full-matrix least-squares techniques with anisotropic thermal displacement parameters for the non-hydrogen atoms converged at $R = 0.0525$, $R_w = 0.1156$, and $S = 1.093$. A difference Fourier synthesis revealed residual densities between -1.096 and $+0.746$ e/Å³. Scattering factors, anomalous dispersion factors and extinction correction used were those supplied in SHELX93. The drawings were made with ORTEP.[19] All calculations were carried out on a μVAX 3400 computer of the Instituto Superior Técnico.

Crystallographic data are summarized in Table 1, final fractional atomic coordinates and equivalent isotropic thermal displacement parameters for non-hydrogen atoms are given in Table 2, and selected bond distances and bond angles are collected in Table 3.

Magnetic Susceptibility. Magnetic susceptibility measurements were performed in the range 4.2–300 K using a longitudinal Faraday system (Oxford Instruments) with a 7 T superconducting magnet. A polycrystalline sample (38 mg) was placed in a thin-wall Teflon bucket, previously measured. The magnetic field used was 2 T, and force was measured with a microbalance (Sartorius S3D-V) applying forward and reverse gradients of 5 T/m. The magnetization was found to be proportional to the applied magnetic field up to 4 T and in the temperature range of the measurements. Paramagnetic susceptibility was calculated from the raw susceptibility data correcting for diamagnetism, that was estimated from tabulated Pascal's constants[20] as 5.60 $\times 10^{-4}$ emu/mol.

(17) Sheldrick, G. M., SHELX 86, Program for Crystal Structure Solution. University of Göttingen, 1986.
(18) Sheldrick, G. M., SHELX93, Program for Crystal Structure Solution. University of Göttingen, 1993.
(19) Johnson, C. K. *ORTEP II*; Report ORNL-5138; Oak Ridge National Laboratory: Oak Ridge, TN, 1976.
(20) Kahn, O. *Molecular Magnetism*; VCH Pub., Inc.: New York, 1993.

Table 2. Atomic Fractional Coordinates ($\times 10^4$) and Equivalent Isotropic Displacement Parameters (Å² $\times 10^3$) for $[(C_2H_5)_4N]_2Cu_5Cl_{12}$

atom	x	y	z	$U_{eq}{}^a$
Cu(1)	0	5000	0	30(1)
Cu(2)	332(1)	2027(1)	236(1)	31(1)
Cu(3)	3218(1)	342(1)	−113(1)	31(1)
Cl(1)	1977(2)	4858(2)	1708(2)	47(1)
Cl(2)	1497(2)	7454(2)	1298(2)	39(1)
Cl(3)	1547(2)	1163(2)	−1397(2)	38(1)
Cl(4)	2240(2)	1434(2)	1648(2)	42(1)
Cl(5)	5393(2)	226(2)	1588(2)	39(1)
Cl(6)	1157(2)	−2247(1)	−1565(2)	34(1)
N	2573(5)	3573(5)	6316(5)	33(1)
C(1)	783(7)	2625(7)	5078(7)	46(1)
C(2)	2513(7)	4677(6)	7764(6)	43(1)
C(3)	3465(7)	4296(7)	5777(8)	47(1)
C(4)	3519(8)	2623(7)	6663(7)	47(1)
C(5)	4166(8)	5945(7)	8998(7)	50(2)
C(6)	2767(9)	5358(8)	5499(8)	56(2)
C(7)	−369(8)	1907(8)	5466(9)	61(2)
C(8)	3703(10)	1446(8)	5364(10)	74(2)

^{a} The equivalent isotropic factor, U_{eq}, is defined as one-third of the trace of the orthogonalized $\mathbf{U}_{ij}$ tensor.

Table 3. Selected Bond Lengths (Å) and Angles (deg) for $[(C_2H_5)_4N]_2Cu_5Cl_{12}{}^a$

Cu(1)−Cl(1)	2.2268(13)	Cu(2)−Cl(4)	2.3165(14)
Cu(1)−Cl(2)	2.2941(14)	Cu(3)−Cl(3)	2.3091(13)
Cl(1)−Cu(2)	2.635(2)	Cu(3)−Cl(4)	2.2851(14)
Cu(2)−Cl(2a)	2.3054(14)	Cu(3)−Cl(5)	2.3029(14)
Cu(2)−Cl(6b)	2.2512(13)	Cu(3)−Cl(5c)	2.2816(13)
Cu(2)−Cl(3)	2.3064(13)	Cu(3)−Cl(6)	2.535(2)

Cl(1)−Cu(1)−Cl(2)	89.38(5)	Cu(2)−Cl(3)−Cu(3)	94.28(5)
Cl(1)−Cu(1)−Cl(2a)	90.62(5)	Cu(2)−Cl(4)−Cu(3)	94.65(5)
Cu(1)−Cl(1)−Cu(2)	90.61(5)	Cl(3)−Cu(3)−Cl(4)	85.53(5)
Cu(1)−Cl(2a)−Cu(2)	97.88(5)	Cl(3)−Cu(3)−Cl(5)	163.24(6)
Cl(1)−Cu(2)−Cl(6b)	96.44(5)	Cl(3)−Cu(3)−Cl(5c)	92.53(5)
Cl(1)−Cu(2)−Cl(2a)	80.87(5)	Cl(3)−Cu(3)−Cl(6)	97.76(5)
Cl(1)−Cu(2)−Cl(3)	98.30(5)	Cl(4)−Cu(3)−Cl(5)	90.95(5)
Cl(1)−Cu(2)−Cl(4)	99.98(5)	Cl(4)−Cu(3)−Cl(5c)	167.11(6)
Cl(2a)−Cu(2)−Cl(3)	91.04(5)	Cl(4)−Cu(3)−Cl(6)	97.18(5)
Cl(2a)−Cu(2)−Cl(4)	175.91(5)	Cl(5)−Cu(3)−Cl(5c)	87.25(5)
Cl(2a)−Cu(2)−Cl(6b)	93.03(5)	Cl(5)−Cu(3)−Cl(6)	98.94(5)
Cl(3)−Cu(2)−Cl(4)	84.88(5)	Cl(5c)−Cu(3)−Cl(6)	95.71(5)
Cl(3)−Cu(2)−Cl(6b)	165.15(6)	Cu(3)−Cl(5)−Cu(3c)	92.75(5)
Cl(4)−Cu(2)−Cl(6b)	90.85(5)	Cu(2b)−Cl(6)−Cu(3)	103.27(5)

^{a} Symmetry transformations used to generate equivalent atoms: a $(-x, -y + 1, -z)$; b $(-x, -y, -z)$; c $(-x + 1, -y, -z)$.

Results and Discussion

Crystal Structure. The crystal structure of $[(C_2H_5)_4N]_2Cu_5$-Cl_{12} consists of two-dimensional $[(Cu_5Cl_{12})^{2-}]_\infty$ networks, parallel to the *a,b* plane (Figure 1), alternating with layers of discrete tetraethylammonium cations along *c* (Figure 2). The anionic sheets can be seen as built up from infinite $(Cu_5Cl_{12})_n{}^{2-}$ zigzag chains interlinked *via* short semicoordinative Cu−Cl bonds. The distance between these interchain links and the undulating nature of the chains originates holes in the $[(Cu_5Cl_{12})^{2-}]_\infty$ sheets (Figure 1). A net charge 2− corresponds to each hole, which is compensated by two equivalent $(C_2H_5)_4N^+$ cations sitting above and below each hole. These two cations are related by an inversion center located in the midpoint of the hole having one of the ethyl groups pointing toward the hole (Figure 2).

The asymmetric unit contains three crystallographically independent copper atoms, six chlorine atoms and one $(C_2H_5)_4N^+$ cation. The chains are made from the repeat Cu(1)−Cu(2)−Cu(3)−Cu(3c)−Cu(2c). This sequence can be viewed as the sum of two sub-sequences: a tetranuclear centrosymmetric Cu(2)−Cu(3)−Cu(3c)−Cu(2c) subunit and a single Cu(1) unit,
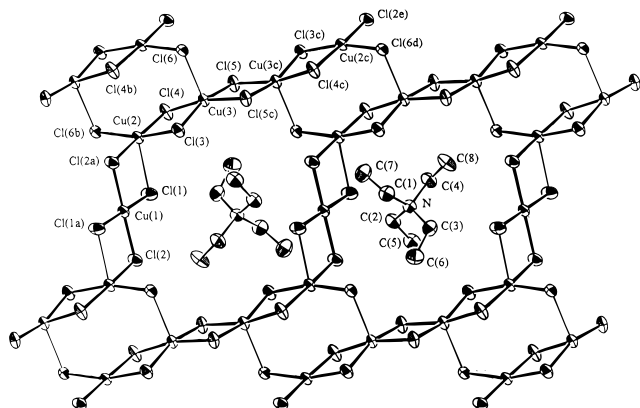
Figure 1. ORTEP projection along the *c* axis of the $[(C_2H_5)_4N]_2Cu_5$-Cl_{12} structure showing the labeling scheme for the atoms. Hydrogen atoms are omitted and only one tetraethylammonium cation on each side of the $[(Cu_5Cl_{12})^{2-}]_\infty$ layer is represented for clarity. Symmetry key: a $(-x, -y + 1, -z)$; b $(-x, -y, -z)$; c $(-x + 1, -y, -z)$; d $(1 - x, y, z)$; e $(1 + x, y - 1, z)$.
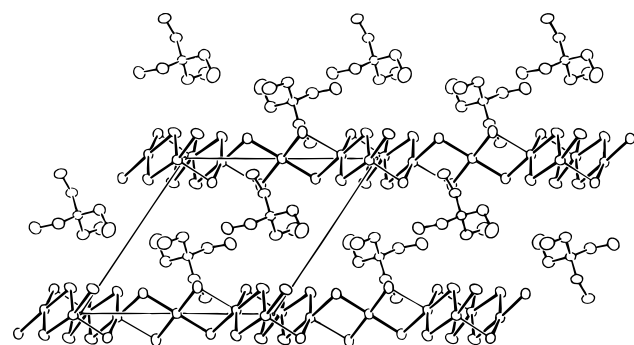

Figure 2. ORTEP projection along the *a* axis of the $[(C_2H_5)_4N]_2Cu_5$-Cl_{12} structure. Hydrogen atoms are omitted for clarity.

which acts as a spacer between tetramers. The chains are constructed alternating these two subunits.

The copper atom of the mononuclear subunit, Cu(1), lies at an inversion center and is four coordinated, so its coordination geometry is planar by symmetry, and almost perfectly square planar (Cu(1)−Cl(1) = 2.2268(13) Å; Cu(1)−Cl(2) = 2.2941(14) Å; Cl(1)−Cu(1)−Cl(2) = 89.38(5)°). Cl(2) bridges symmetrically the Cu(1) with the adjacent Cu(2); Cl(1) bridges asymmetrically the same copper pairs. The other four copper atoms of each sequence, Cu(2)−Cu(3)−Cu(3c)−Cu(2c), define the core of a pseudoplanar tetrameric subunit. This subunit includes the 10 chlorine atoms linked by normal Cu−Cl bonds (the average Cu−Cl length is ∼2.3 Å) to the core copper atoms; six of them bridge adjacent copper atoms into the tetramer (Cl(3), Cl(4), Cl(5), Cl(5c), Cl(4c), and Cl(3c)), and the other four (Cl(2a), Cl(6b), Cl(2e), and Cl(6d)) are located in the edges (Figure 1). The two equivalent Cl(6) moieties in a tetramer are implicated in the interchain semicoordinative bonds (Cu(3)−Cl(6), 2.535(2) Å), responsible for the chain aggregation that builds up the two-dimensional network. The atoms linked by these short semicoordinative bonds present the larger deviations from the least square plane of the tetramer (Cu(3), 0.264 Å; Cl(6b); 0.229 Å).

Although being integrated in an infinite chain, the tetrameric subunit has a configuration that resembles the discrete pseudoplanar tetramers present in $[(CH_4)_4N]_2Cu_4Cl_{10}$ and $(4MAP)_2Cu_4$-Cl_{10}[12] (4MAP, 4-methyl-2-aminopyridinium). In the title compound interior Cl−Cu−Cl bonds angles are all less than 90°, as typically observed in the pseudoplanar oligomers. The magnetically important bridging Cu−Cl−Cu angles are 92.75(5)° for the central Cu(3)−Cl(5)−Cu(3c) and 94.28(5) and 94.65(5)° for the terminal Cu(2)−Cl(3)−Cu(3) and Cu(2)−Cl(4)−Cu(3)

respectively. These values are very similar to those, close to 94°, observed in the compounds with discrete tetramers.[12] Finally, it should be noted that while in the discrete tetranuclear compounds the $(Cu_4Cl_{10})^{2-}$ are linked in stacks by semicoordinative bonds, in the title compound, the chain aggregation consists of stacking along *a* of the tetrameric segments belonging to adjacent chains. If the notation of Willett et al.[14] were applicable to the nondiscrete tetramers of our compound, it would correspond to a $4(^5/_2, {}^1/_2)$ stacking pattern. As the least-square plane of the tetramer is almost perpendicular (86.98(4)°) to the plane defined by the mononuclear subunits (Cu(1), Cl(1), Cl(2)), the Cu(1) atoms are not allowed to collaborate in the interchain connection. The large distance between different Cu(1) atoms, separated by the holes in the anionic sheets, also avoids any interchain interaction via these atoms.

The two independent copper atoms in the tetramer (Cu(2) and Cu(3)) present different geometry of coordination. Cu(2) has a distorted (4 + 1) pyramidal coordination. The Cu−Cl bonds belonging to the tetrameric subunit are in the range 2.25-2.32 Å while the apical Cl(1)−Cu(2) bond is nearly orthogonal to the four former bonds, with a length of 2.635(2) Å, denoting a semicoordinative nature. The stacking of the tetramers leads also to a longer semicoordinative Cu−Cl contact between adjacent chains; Cu(2)−Cl(4b) 3.34 Å (not represented in Figure 1), so the Cu(2) coordination can be seen as 4 + 1 + 1. The coordination geometry about Cu(3) is very close to elongated square pyramidal, with basal Cu−Cl bonds distances in the range 2.28−2.31 Å and an apical Cu(3)−Cl(6) distance of 2.535(2) Å. Cu(3) remains 0.30 Å above the plane of the four basal chlorine atoms. The distances and angles observed in the $(C_2H_5)_4N^+$ cation are normal (N−C = 1.501(7)−1.542(7) Å; C−N−C′ = 107.1(4)−112.5(4)°).

The preservation of a substantial portion of the $CuCl_2$ structure in many of the structures for copper(II) halide salts have been noticed frequently.[2] The $CuCl_2$ layered structure, as depicted in Figure 3a, is made up of infinite bibridged $-(CuCl_2)_\infty-$ chains with the Cu−Cl bond distances of approximately 2.30 Å, aggregated by interchain semicoordinative Cu−Cl bonds (≈ 3.0 Å).[21]

The structures of the wide class of pseudoplanar bibridged oligomeric compounds with formula $(Cu_nCl_{2n+2})^{2-}$ (as well as their bromide analogues) can be viewed as obtained by segmentation of the infinite $(CuCl_2)_\infty$ chains in the parent $CuCl_2$ structure when pairs of halide ions are periodically inserted along the chain. Sometimes the stacking pattern maintains a close relationship with the parent $CuCl_2$ structure, and the stack then consists of a simple slab of the $CuCl_2$ structure. However, different variations are frequently introduced at this point, giving rise to a larger diversity of structures. As an example, the $[CH_3N(C_2H_5)_3]Cu_3Cl_7$ structure[2] is representative of another way to modify the $CuCl_2$ structure: the removal of positive fragments. The anionic sheets of this compound correspond to the removal of $(Cu_2Cl_2)^{2+}$ fragments at periodical intervals along alternating chains of the parent $CuCl_2$ structure. The $[(CH_3)_4$-$P]Cu_2Cl_5$[22] and $[(CH_3)_4As]Cu_2Cl_5$[23] isomorphous structures also could be generated by removal of $(Cu_2Cl_2)^{2+}$ fragments, but here the higher density of holes produces more severe distortions, and as a consequence many characteristics of the parent structure, in particular the ferrodistortive nature of the elongated axes of the coordination polyhedra, are lost.

In Figure 3a−c we show how the structure of the title compound can be derived from the $CuCl_2$ structure by periodic

(21) Wells, A. F. *J. Chem. Soc.* **1947**, 1670.
(22) Haije, W. G.; Dobbelaar, J. A. L; Maaskant, W. J. A. *Acta Crystallogr., Sect C* **1986**, *C42*, 1485.
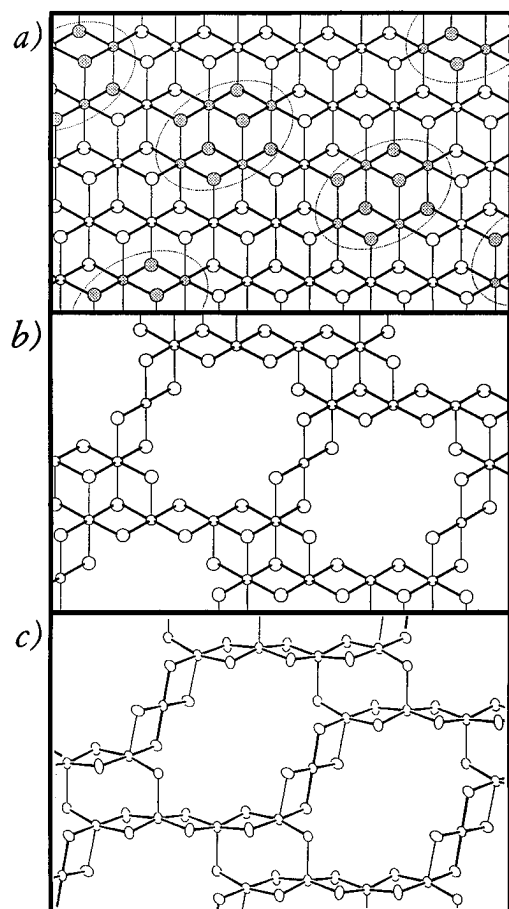(23) Murray, K; Willett, R. D. *Acta Crystallogr., Sect C* **1993**, *C49*, 1739.

Figure 3. Relation of the chlorocuprate structure in [(C$_2$H$_5$)$_4$N]$_2$Cu$_5$-Cl$_{12}$ to the parent CuCl$_2$ structure: Cl, larger circles; Cu, smaller circles. Key: (a) Representation of the CuCl$_2$ structure, with bibridged chains running horizontally. Semicoordinative linkages between chains are visualized by vertical dashed lines. The dotted ellipsoids mark the (Cu$_4$-Cl$_6$)$^{2+}$ fragments that must be removed to generate the [(Cu$_5$Cl$_{12}$)$^{2-}$]$_\infty$ network structure. (b) Ideal structure after removal of (Cu$_4$Cl$_6$)$^{2+}$ fragments from the CuCl$_2$ network. (c) Real chlorocuprate network in the [(C$_2$H$_5$)$_4$N]$_2$Cu$_5$Cl$_{12}$ structure.

elimination of larger (Cu$_4$Cl$_6$)$^{2+}$ fragments (indicated in Figure 3a by dashed ellipsoids). These fragments, like the fragments eliminated in the other three referred structures with holes, have 2+ charge. In this respect it is worth noting that Willett et al.[2] suggested that since it is not possible to pack more than two cations about each hole the removal of fragments with higher charge would be energetically unfavorable.

The structure obtained by simply omitting the (Cu$_4$Cl$_6$)$^{2+}$ fragments is represented schematically in Figure 3b. Obviously many distortions are necessary to stabilize the resulting network, but it is remarkable how this ideal intermediate structure contains already the same number of independent copper and chlorine atoms and the same basic geometry as in the final real structure (Figure 3c). The original bibridged chains (running horizontally in Figure 3a) are disrupted after fragment removal, producing tetramers and monomers. The most significant modification from Figure 3b, in order to approach the real structure (Figure 3c), is the shortening, to a normal Cu−Cl bond distance, of the primitive semicoordinative bonds about the copper arranged as isolated monomer. This shortening satisfies the four-coordination requirement of this copper atom that otherwise were unfulfilled after the fragment removal. This process generates new infinite chains, now running along a diagonal in Figure 3c.

A simple mechanism explains the other modification; while in the CuCl$_2$ structure each chlorine atom is implicated in two normal and one semicoordinative Cu−Cl bonds, in our new
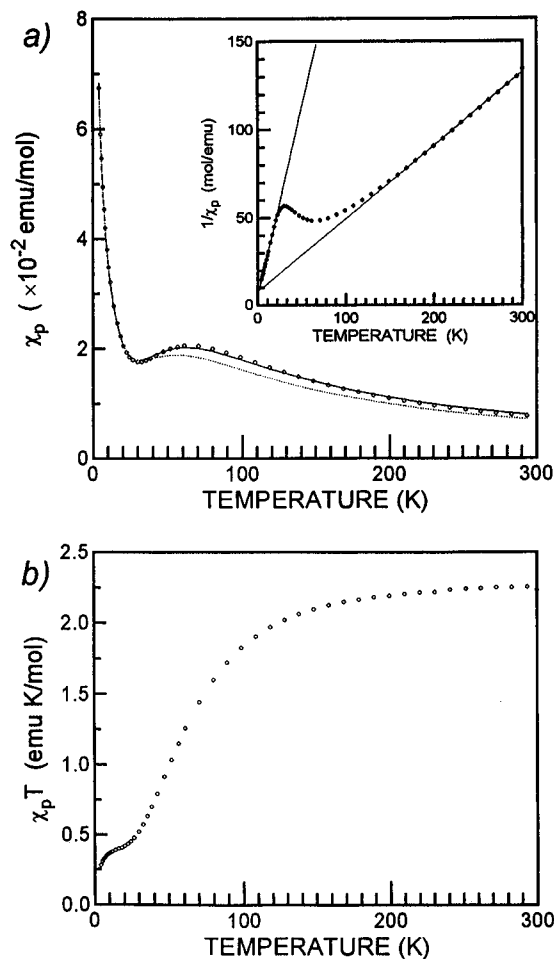

Figure 4. Experimental paramagnetic susceptibility, χ_p, of [(C$_2$H$_5$)$_4$N]$_2$-Cu$_5$Cl$_{12}$ (a). and the $\chi_p T$ product (b) as a function of temperature. The line in part a is the best fit of eq 1 (see text); the inset shows the plot of χ_p^{-1} vs T.

network, the chlorine atoms that had lost one normal Cu−Cl bond, reinforce the remaining semicoordinative bond, so its length is noticeably reduced down from the original 3 Å (Cu(2)−Cl(1), 2.635(2) Å; Cu(3)−Cl(6), 2.535(2) Å). As a consequence, the opposite semicoordinative bond of copper atoms affected by this modification is significantly elongated, becoming almost negligible for Cu(2) (Cu(2)−Cl(4b), 3.34 Å) and disappears in Cu(3).

The square planar coordination geometry of Cu(1) denotes that the electrostatic repulsion between chlorides, favoring a tetrahedral geometry, is reduced due to the bridging nature of all the chloride ions bonded to it. This "charge compensation" effect[2] allows the dominance of the crystal field effects that favors a square planar geometry. This is further helped by the blocking of the two vacant semicoordinative positions by the (C$_2$H$_5$)$_4$N$^+$ cation presenting two distances Cu−C of 3.80 Å (Cu(1)−C(2f) and Cu(1)−C(2g); *f*(*x*, *y*, −1 + *z*), *g*(−*x*, 1−*y*, 1 − *z*)). The vacant semicoordinative position of Cu(3) is also blocked by the same ethyl group (distance Cu(3)−C(5h) 3.86 Å, *h*(1 − *x*, 1 − *y*, 1 − *z*)). The blockage of the vacant semicoordinative positions by the alkyl group of the cations, a characteristic also present in the three other reported two-dimensional chlorocuprate structures with holes, stabilizes the structure.

The title compound has a structure distinctly different from (C$_2$H$_5$)$_4$NCu$_4$Cl$_{12}$, another previously known tetraethylammonium halocuprate, with discrete tetranuclear anions.[24] This shows that, although the coordination geometry of the chlorocuprates is strongly dependent both on cation size and on

possible hydrogen bonding effects, the preparative conditions are also determinant to the structure.

Magnetic Behavior. The temperature dependence of the paramagnetic susceptibility, χ_p, is depicted in Figure 4a. When the complex is cooled from room temperature, the susceptibility passes through a broad maximum at about 65 K and a local minimum at about 32 K and then increases, approximately as a Curie law, until the lowest temperature measured. As shown in Figure 4b, the $\chi_p T$ product curve exhibits a continuous decreasing upon cooling denoting that the ground state is dominated by antiferromagnetic interactions. However this decrease occurs in two steps: at room temperature $\chi_p T$ approaches the value corresponding to an effective magnetic moment of 4.24 μ_B, and between 22 and 8 K there is a plateau corresponding to an effective magnetic of $\approx$1.8 μ_B, close to the moment due to an $S = {}^1\!/_2$ spin by the spin-only formula, 1.73 μ_B.

The low temperature tail in susceptibility cannot be seen as only due to a small fraction of impurities or defects. In fact, as shown by the χ_p^{-1} versus T plot (inset Figure 4a), for T < 20 K, data closely follow a Curie–Weiss law with $C' = 0.466(1)$ emu K/mol, corresponding to about one $S = {}^1\!/_2$ spin per formula unit, and $\Theta' = -2.69(5)$ K. For $T > 150$ K a different Curie–Weiss law is approached, with $C = 2.43(1)$ emu K/mol and $\Theta = -21.6(9)$ K. The relation C/C' is approximately 5 (5.17) suggesting that larger antiferromagnetic interactions affect four out of each five copper atoms, and from these only one maintains a relevant contribution to the susceptibility at the lower temperatures. This fact is taken as a direct consequence of the structure of this compound, in which, as previously described, the five copper atoms per stoichiometric formula can be considered as arranged in tetramers and monomers.

Since there is not a detailed model for our complex two-dimensional network of tetramers and monomers, we tried, as a first approximation, to reproduce the susceptibility of this compound by a simple model that considers the global susceptibility, χ_p, as the sum of two independent contributions, one due to tetramers of $S = {}^1\!/_2$ spins, $(\chi_p)_t$, and the other due to monomers, $(\chi_p)_m$, in addition to a possible temperature independent term A.

$$\chi_p = (\chi_p)_t + (\chi_p)_m + A \tag{1}$$

The $(\chi_p)_t$ contribution is expected to be the one derived from the nearest neighbor Heisenberg Hamiltonian for a linear $S = {}^1\!/_2$ tetramer,

$$\mathcal{H} = -2J_1(\vec{S}_1\vec{S}_2 + \vec{S}_3\vec{S}_4) - 2J_2(\vec{S}_2\vec{S}_3) \tag{2}$$

where J_1 is the exchange constant between edge and central copper atoms and J_2 is the coupling between the central copper atoms, all considered as spins $S = {}^1\!/_2$. This model has an exact solution previously described,[25] and considering a unique g value for the four copper ions, it gives a magnetic susceptibility as

$$(\chi_p)_t = (N_0 g^2 \mu_B^2/kT)[10\exp(-E_1/kT) + 2\exp(-E_2/kT) + 2\exp(-E_3/kT) + 2\exp(-E_4/kT)/Z] \tag{3}$$

$$Z = 5\exp(-E_1/kT) + 3(\exp(-E_2/kT) + \exp(-E_3/kT) + \exp(-E_4/kT)) + \exp(-E_5/kT) + \exp(-E_6/kT)$$

where E_n are the energy levels with spin quantum numbers S_n given in ref 25.

The $(\chi_p)_m$ contribution is expected to follow a Curie–Weiss model for $S = {}^1\!/_2$ spins:

$$(\chi_p)_m = N_0 g^2 \mu_B^2/4k(T - \Theta) \tag{4}$$

The best fit of our data with eq 1 (the solid line in Figure 4a) was obtained for $J_1/k = -64(2)$ K, $J_2/k = 20(38)$ K, $g_t = 2.44(4)$, $g_m = 2.20(3)$, $\Theta = -2.7(8)$ K, and $A = 0.0001(2)$ emu/mol, where g_t and g_m are the g values used in eqs 3 and 4, respectively. The J_1/k, J_2/k values corresponding to our tetramer are very similar to those estimated for the discrete $(Cu_4Cl_{10})^{2-}$ tetramers of the tetramethylammonium and 4-methyl-2-aminopyridinium salts.[12] In these compounds the antiferromagnetic coupling of the pairs of outer copper atoms in the tetramer, J_1/k, was estimated as -59.2 (9) and $-62.1(2)$ K, respectively, while J_2/k was estimated with larger uncertainties as 26(18) and 36(32) K. The A value is quite small, on the order of those estimated for other halocuprates.[4,11,12] Although similar values have been also reported for other Cu(II) compounds,[26] the g value of the tetramer, g_t, is quite large and considered unrealistic. If we consider more realistic values imposing an upper limit to g_t as 2.2, a poorer fit was obtained (dotted line in Figure 4a) with $J_1/k = -63(10)$ K, $J_2/k = 43(140)$ K, $g_t = 2.2(1)$, $g_m = 2.10(6)$, $\Theta = -3(3)$ K, and $A = 0.0009(6)$ emu/mol. However it is worth noting that the stronger deviations in this fitting are obtained only above $\sim$30 K whereas below this temperature the fit is equally good.

It is remarkable how, in spite of the Cu(1)–Cu(2) distance (3.47 Å) being similar to the Cu(2)–Cu(3) distance (3.385 Å) of the strongly coupled spins of the tetramers, both with two chloride ions bridging, the Cu(1) spins in this structure appear magnetically so isolated from the remaining copper atoms, as denoted by the rather small Weiss constant, $\Theta = -2.7(8)$ K. This fact denotes the anisotropic nature of the magnetic coupling between copper(II) spins, which is indirectly bridged by the chlorine atoms. While the tetramer least-square planes roughly include the coupled copper atoms (Cu(2), Cu(3)), their bridging chlorine atoms (Cl(3), Cl(4)), and also the other strongly coordinating chlorides of both copper atoms, the coordination plane of Cu(1) is almost perpendicular to the average plane of the tetramer.

In conclusion $[(C_2H_5)_4N]_2Cu_5Cl_{12}$ presents a new case of a rare structural type among halocuprates(II), related to the CuCl2 structure by removal of dipositive fragments. Its structure consists of chlorocuprate layers alternating with layers of discrete cations. The chlorocuprate layers are built up from pseudoplanar tetranuclear and almost orthogonal mononuclear subunits. The magnetic susceptibility clearly reflects the distinct contributions of these two subunits.

Supporting Information Available: Tables listing detailed experimental data for X-ray diffraction, complete bond distances and bond angles and anisotropic displacement parameters of non-hydrogen atoms, derived hydrogen coordinates and isotropic displacement parameters, and least-square planes (5 pages). Ordering information is given on any current masthead page.

IC9505864

(24) Willett, R. D.; Geiser, U. *Inorg. Chem.* **1986**, *25*, 4558.
(25) Rubenacker, G. V; Drumheller, J. E, Emerson, K, Willett, R. D. *J. Magn. Magn. Mater.* **1986**, *54–57*, 1483.

(26) Neels, A.; Stoeckli-Evans, H.; Escuer, A.; Vicente, R. *Inorg. Chem.* **1995**, *34*, 1946.